Applied Physics A (2018) 124:228
https://doi.org/10.1007/s00339-018-1656-8

Applied Physics A
Materials Science & Processing

Activation of dopant in silicon by ion implantation under heating sample at 200 °C

Toshiyuki Sameshima[1] · Keisuke Yasuta[1] · Masahiko Hasumi[1] · Tomokazu Nagao[2] · Yutaka Inouchi[2]

Received: 27 November 2017 / Accepted: 5 February 2018

Abstract
Activation and carrier generation are reported in the case of phosphorus implantation with a dose of 2.0×10^{15} cm^{-2} at 70 keV to crystalline silicon substrates under heating ranging from 200 to 500 °C. The analysis of the optical reflectivity spectra of implanted surfaces revealed that the effective amorphized thickness was low of 2.9 nm in the case of 200 °C-phosphorus implantation, while it was large of 140 nm for implantation at room temperature. The carrier density par unit area increased from 6.9×10^{13} to 4.8×10^{14} cm^{-2} and the photo-induced minority carrier effective lifetime increased from 2.2×10^{-6} to 1.6×10^{-4} s as the implantation temperature increased from 200 to 500 °C. Defect reduction with 1.3 MPa H_2O vapor heating at 250 °C for 3 h increased the carrier density par unit area of the 200 °C-phosphorus-implanted sample to 2.7×10^{14} cm^{-2}. The rectified characteristics were obtained by current–voltage measurement in the case of phosphorus implantation to p-type silicon substrate. Photovoltaic effect was also observed. These results show that the ion implantation under low temperature heating has a capability of p–n junction formation.

1 Introduction

Low temperature fabrication technology of semiconductor devices is important to reduce thermal budget. Low thermal budget process reduces tact time of device fabrication. It realizes low cost production of semiconductor devices. Especially, low temperature fabrication technology is important to fabricate thin film transistors, photo sensors, and solar cells on no thermally resistive materials, for example, glass and plastic substrates. Activation has been a serious problem for the ion implantation technology. Post-annealing above 800 °C is necessary for activation in general [1–4] because thermal energy requires to move implanted dopant atoms from interstitial sites to the lattice sites. The technology of substrate heating during ion-implantation is attractive for recrystallization and activation of implanted region [5, 6].

In this paper, we demonstrate an activation behavior in implanted region of silicon via analyses of crystalline and electrical properties in the case of phosphorus implantation under substrate heating from 200 to 500 °C [7]. Effective recrystallization and a few residual disordered regions are demonstrated via analysis of optical reflectivity spectra. Decrease in the sheet resistivity and increase in the carrier density are then reported with results of microwave-free carrier absorption. Defect passivation is also discussed to decrease the sheet resistivity and increase the carrier density. A high photo-induced minority carrier effective lifetime is also reported by the method of microwave photo-induced free carrier absorption. The rectified diode characteristics is demonstrated by current–voltage measurement for p-type silicon samples implanted with phosphorus atoms under substrate heating from 200 to 500 °C. Photovoltaic effect is also demonstrated in the case of air mass 1.5 light illumination at 0.1 W cm^{-2}.

2 Experimental

We prepared 4-inch-sized single crystalline silicon substrates with a preferential orientation of (100) and a resistivity higher than 4000 Ω cm in order to investigate carrier generation and minority carrier recombination properties by ion implantation. Phosphorus atoms were then implanted at an acceleration energy of 70 keV with a dose of 1×10^{15} cm^{-2} at 200, 300, 400 and 500 °C and room temperature (RT) to

✉ Toshiyuki Sameshima
tsamesim@cc.tuat.ac.jp

[1] Tokyo University of Agriculture and Technology, Tokyo 184-8588, Japan

[2] Nissin Ion Equipment Co. Ltd., Shiga 528-0068, Japan

Published online: 09 February 2018

the top and rear both surfaces of the high resistivity, crystalline silicon samples. The total dose of phosphorus atoms was therefore 2×10^{15} cm^{-2} for each sample. Calculation with the program of transportation of ion in material (TRIM) [8] resulted in that the phosphorus in-depth profile had peaks at 100 nm. Most of the atoms were incorporated within 200 nm surface region. The 0.9-MPa-H_2O-vapour-heat treatment for 3 h at 250 °C was applied to the as-implanted samples for the purpose of defect passivation [9]. 4-inch-sized single p-type crystalline silicon substrates with a preferential orientation of (100) and a resistivity of 10 Ω cm were also prepared to investigate p–n junction formation. Phosphorus atoms were implanted to the top surface at 70 keV with a dose of 1×10^{15} cm^{-2} at 200 and 500 °C.

Optical reflectivity spectra were measured at the implanted surfaces between 250 and 1000 nm using a conventional spectrometer to investigate crystalline volume ratio in the implanted region. The optical reflectivity spectra were analyzed using a numerical calculation program, which was developed with the optical interference effect for a structure of air/seven Si layers/crystalline silicon substrate [10, 11]. The optical reflectivity depends on the complex refractive indexes of silicon. Using the effective dielectric media approximation, the complex refractive index with a crystalline volume ratio X was determined by combing the refractive index of crystalline silicon [12] n_c with the refractive index of amorphous silicon [13] n_a as,

$$n_f = Xn_c + (1 - X)n_a. \quad (1)$$

The values of the parameters of thickness and X were changed each layer to search a reflectivity spectrum which best agreed with experimental spectra. The most possible in-depth distribution of X was then obtained.

To investigate the electrical conductivity and carrier lifetime, we used a 9.35-GHz-microwave-transmittance measurement system [14, 15]. The system had waveguide tubes, which had a narrow gap where a sample was placed. Continuous-wave (CW) 635 nm laser diode (LD) light with a penetration depth of 2.7 μm was introduced into the waveguide tubes. The light intensities were set at 0.74 mW cm^{-2} on the sample surface for 635 nm lights. The microwave transmittance in a dark field T_d was detected to obtain the sheet resistivity. A finite-element numerical calculation program was made with a Fresnel-type microwave interference effect between silicon surfaces and the free carrier absorption to estimate the sheet resistivity, which was obtained by fitting the calculated T_d to the experimental T_d. The microwave transmittance under the light illumination of the ion-implanted surface T_p was also measured to obtain the photo-induced minority carrier effective lifetime τ_{eff}. τ_{eff} was analyzed by the numerical program of carrier diffusion and annihilation to estimate the carrier recombination velocity at the implanted surfaces [14].

Optical reflectivity spectra were measured in the infrared region between 400 and 7000 cm^{-1} by Fourier transform infrared spectrometer (FTIR) to investigate the carrier mobility [11]. The sample room was evacuated for accurate measurement by reducing absorption owing to molecular vibrations and rotations. Measurements of transmissivity and reflectivity spectra gave an experimental optical absorbency spectrum. A seven-layered numerical calculation program using free-carrier absorption effect was made for analyzing experimental absorbency spectrum to estimate the carrier mobility [11]. The thickness, carrier density, and carrier mobility were put in each layer. Optical coupling effect among those layers was also considered by optical interference effect. Because the free carrier absorption effect is not sensitive in the infrared range as compared with 9.35 GHz, the sheet resistivity was first determined by the 9.35 GHz microwave transmittance measurement and its analysis for sample implanted at every temperature. The carrier mobility was then estimated by analyzing the infrared absorbency spectrum for the sample with the low sheet resistivity caused by phosphorus implantation at 500 °C. That value of the carrier mobility was used to estimate the carrier density per unit area as a function of implantation temperature from 200 to 500 °C.

Al electrodes were formed on the top surface of the p-type silicon sample, which phosphorus atoms were implanted and also on the rear surface in order to measure current–voltage characteristics. Air mass (AM) 1.5 light were illuminated to the samples at 0.1 W cm^{-2} to investigate photo-induced and photovoltaic characteristics.

3 Results and discussion

Figure 1 shows optical reflectivity spectra of surfaces in the cases of phosphorus implantation at 200 °C (red curve), and RT, and initial bare silicon. The optical reflectivity spectrum for the bare silicon sample shows large E_1 and E_2 peaks appeared at approximately 370 and 275 nm caused by the large joint density of states at the crystal-line in the Brillouin zone of crystalline silicon, while there were no peaks in the spectrum of phosphorus-implanted samples at RT. This means that phosphorus ions caused substantial disordered states in the implanted surface region of crystalline silicon. The sample implanted with phosphorus at 200 °C shows an optical reflectivity spectrum with E_1 and E_2 peaks similar to that for the initial bare silicon sample. This indicates that the crystalline state was well maintained in the phosphorus-implanted region in the case of 200 °C implantation. Similar optical reflectivity spectra were obtained in the cases of phosphorus implantation at 300, 400 and 500 °C. Figure 2 shows in-depth profile of X obtained by fitting calculated reflectivity spectra to experimental spectra

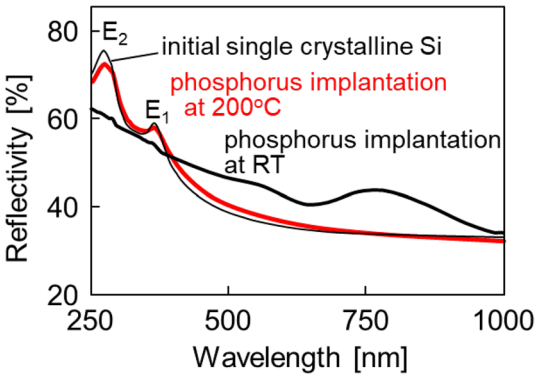

Fig. 1 Optical reflectivity spectra of the sample surfaces in the cases of phosphorus implantation at 200 °C (red curve) and RT, and initial single crystalline silicon

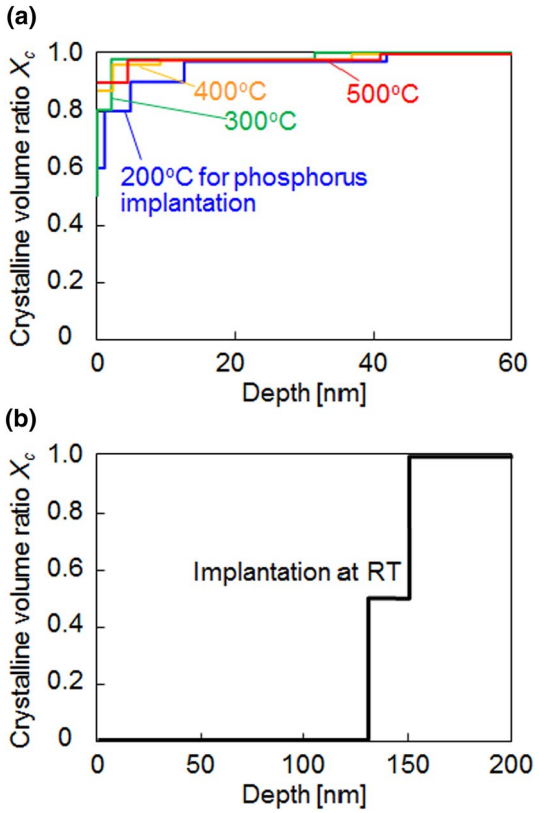

Fig. 2 In-depth profile of X obtained by fitting calculated reflectivity spectra to experimental spectra for **a** phosphorus-implanted samples under heating ranging from 200 to 500 °C and **b** phosphorus sample implanted at RT

for (a) phosphorus-implanted samples under substrate heating ranging from 200 to 500 °C and (b) phosphorus sample implanted at RT. X was low values in the only a top few nm regions in the cases of phosphorus implantation ranging from 200 to 500 °C, as shown in Fig. 2a, while X was zero in the top 130 nm in the case of implantation at RT, as shown in Fig. 2b. The effective amorphized thickness A_{eff} is defined by in-depth integration of $(1-X(x))$ as,

$$A_{\mathrm{eff}} = \int_0^\infty (1 - X(x))\mathrm{d}x. \tag{2}$$

Figure 3 shows A_{eff} as a function of heating temperature during ion implantation (red solid circles). 200 °C-phosphorus implantation resulted in low of A_{eff} of 2.9 nm. A_{eff} decreased to 1.1 nm as the substrate temperature increased to 500 °C. On the other hand, black solid circles show A_{eff} analyzed in the case of phosphorus implantation at RT followed by annealing from 200 to 400 °C in air atmosphere for 1 h. A_{eff} was 140 nm in the as-implanted case at RT. It slightly decreased to 125 nm as the post-annealing temperature increased to 400 °C. Those results of Figs. 1, 2 and 3 clearly show that highly effective recrystallization was realized by phosphorus implantation under substrate heating between 200 and 500 °C.

Figure 4 shows the sheet resistivity estimated by 9.35 GHz microwave transmission method as a function of the substrate temperature for the samples as-phosphorus implanted under substrate heating (red solid circles), additionally treated with high pressure H_2O vapor heat treatment (blue solid circles), and phosphorus implanted at RT followed by heated (black solid circles). The sheet resistivity was 3280 Ω sq^{-1} for phosphorus implantation at 200 °C. Because the sheet resistivity of the initial bare silicon substrate was high of 15,000 Ω sq^{-1}, 200 °C-substrate heating during phosphorus implantation caused carrier generation. A part of dopant atoms moved to the silicon lattice sites and generated carriers during ion implantation under substrate heating. The sheet resistivity decreased to 470 Ω sq^{-1} as the substrate temperature increased to 500 °C during implantation, as shown by red solid circles. The activation ratio

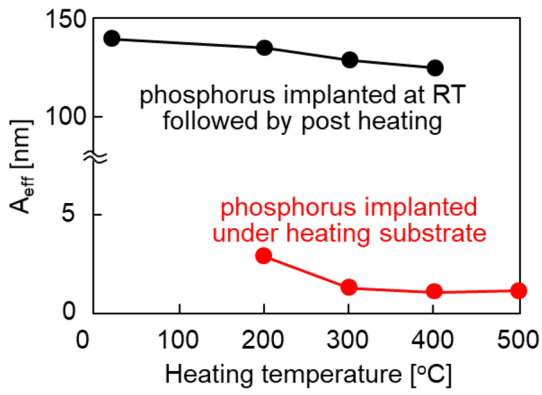

Fig. 3 A_{eff} as a function of heating temperature during ion implantation (red solid circles) and as a function of the post-annealing temperature for implantation at RT (black solid circles)

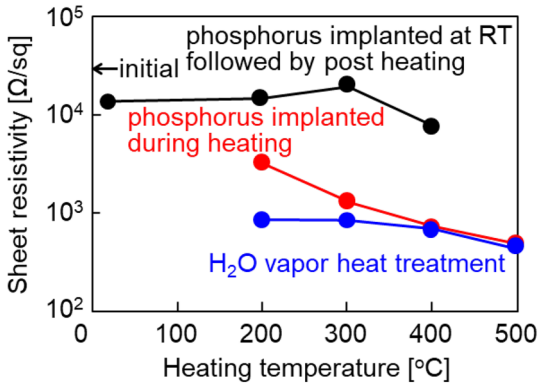

Fig. 4 Sheet resistivity as a function of the temperature of substrate heating during phosphorus implantation for as-implanted samples (red solid circles) and samples with additional 0.9 MPa H_2O vapor heat treatment at 250 °C for 3 h (blue solid circles). The sheet resistivity as a function of the post-annealing temperature for implantation at RT is also plotted by (black solid circles)

effectively increased as the substrate temperature increased to 500 °C. The additional high pressure H_2O vapor heat treatment at 250 °C for 3 h markedly decreased the sheet resistivity to 858 Ω sq^{-1} in the case of 200 °C implantation. Moreover, the sheet resistivity decreased to 436 Ω sq^{-1} as the temperature during implantation increased from 200 to 500 °C, as shown by blue solid circles. Decrease in the sheet resistivity probably results from reduction of defect states which trapped carriers generated from activated phosphorus atoms. On the other hand, the sheet resistivity was very high of 12,000 Ω sq^{-1} for as-implanted sample at RT. It was hardly changed by post-annealing up to 400 °C in air atmosphere for 1 h, as shown by black solid circles.

Figure 5 shows the experimental optical absorbency spectrum by a red curve in the case of as-phosphorus implantation at 500 °C measured by FTIR. Calculated optical absorbency spectra with different carrier mobilities are also shown by black curves. The optical absorbency increased as the wave-number decreased because the light with low frequency was sensitively absorbed by free carriers in silicon. Spectral shape depended on the carrier mobility. Low mobility showed strong damping with high absorbance over wide range of wavenumber. On the other hand, high mobility showed sharp absorption characteristic limited in the low wavenumber region. The calculated spectrum with a carrier mobility of 27 cm^2 V^{-1} s^{-1} well agreed to the experimental one, as shown in Fig. 5.

The carrier density per unit area was estimated, as shown in Fig. 6, for samples in the cases of as-implanted under substrate heating and additional high pressure H_2O vapor heat treatment at 250 °C with the result of the sheet resistivity shown in Fig. 4 and the carrier mobility of 27 cm^2 V^{-1} s^{-1} shown in Fig. 5. It was 6.9×10^{13} cm^{-2} in the case of as-200 °C-phosphorus implantation. It means that 3.5% phosphorus atoms were activated. The carrier density per unit area increased to 4.8×10^{14} cm^{-2} as the implantation temperature increased to 500 °C. A high activation ratio of 24% was achieved by phosphorus implantation at 500 °C. Although a high crystalline volume ratio was already obtained in the case of 200 °C heating implantation as shown in Figs. 2 and 3, the carrier density was still low. There is a possibility of carrier trapping by the high density of defects caused by 200 °C-phosphorus implantation. The 0.9-MPa H_2O vapor heat treatment at 250 °C for 3 h increased the carrier density for the every implantation temperature case, as shown by blue solid circles in Fig. 6. Especially the carrier density increased from 6.9×10^{13} to 2.7×10^{14} cm^{-2} in the case of 200 °C-phosphorus implantation. The activation ratio increased to 13.5%. This result indicates that substantial carrier-trapping-type defect states were formed in the 200 °C-phosphorus-implanted region. Defect passivation is a problem to achieve a high density of carrier for low

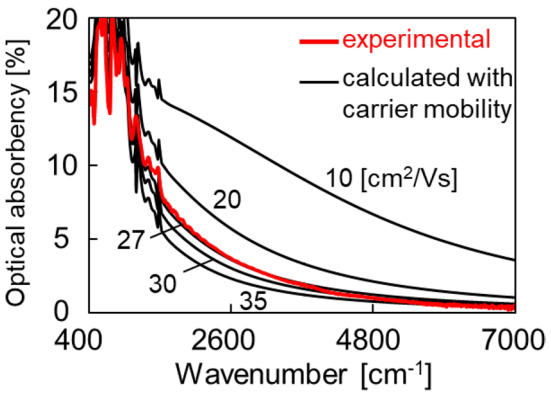

Fig. 5 Experimental optical absorbency spectrum in the case of phosphorus implantation at 500 °C (red curve) and calculated optical absorbency spectra with different carrier mobilities

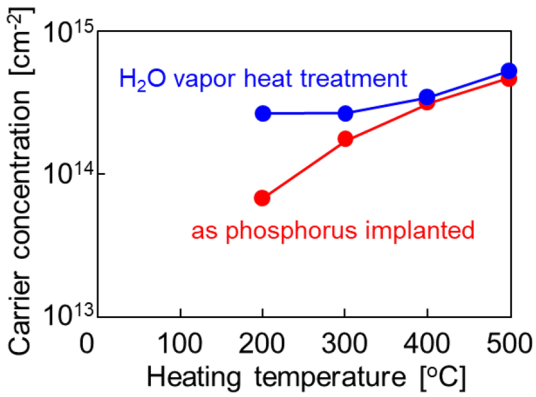

Fig. 6 The carrier density per unit area as a function of implantation temperature for phosphorus-implanted samples (red solid circles) and samples treated in 0.9 MPa H_2O vapor at 250 °C for 3 h (blue solid circles)

temperature implantation. The H_2O vapor heat treatment at 250 °C for 3 h also increased the carrier density par unit area to 5.3×10^{14} cm^{-2} for the case of 500 °C-phosphorus implantation. The activation ratio increased to 27%. H_2O vapor heat treatment was effective for defect passivation for majority carriers.

Figure 7 shows (a) τ_{eff} and (b) the recombination velocity as a function of the temperature of substrate heating during ion implantation for as-implanted samples. τ_{eff} was 1.7×10^{-6} s for phosphorus implantations at 200 °C, which were similar values to τ_{eff} of the initial bare silicon substrate. 200 °C-substrate heating was not effective for passivating the surfaces. τ_{eff} increased to 1.7×10^{-4} s as the substrate temperature increased to 500 °C. Decrease in A_{eff} and increase in carrier density resulted in effective surface passivation. The recombination velocity of the implanted surface was decreased from 1.5×10^4 to 150 cm s^{-1} as the substrate temperature increased from 200 to 500 °C. However, the 0.9 MPa H_2O vapor heat treatment for 3 h at 250 °C hardly changed τ_{eff}. Conditions for reduction of trap defects for majority carrier and recombination defects for minority carrier would be different. Further investigation of defect pasivation is necessary for realizing high effective lifetime and low recombination velocity.

Figure 8 shows plots of electrical current density as a function of applied voltage (J–V) for the 10 Ω cm p-type samples with the top surface implanted with phosphorus atoms at (a) 200 and (b) 500 °C under the conditions of the dark field and AM 1.5 light illumination at 0.1 W cm^{-2} to the

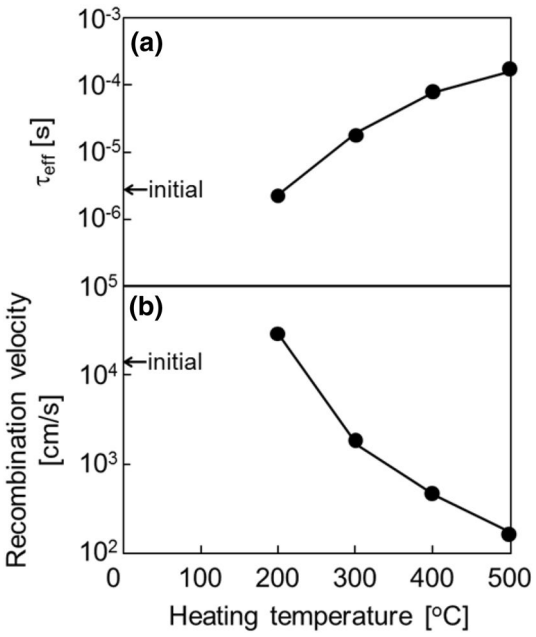

Fig. 7 **a** τ_{eff} and **b** the recombination velocity as a function of the temperature of substrate heating during ion implantation

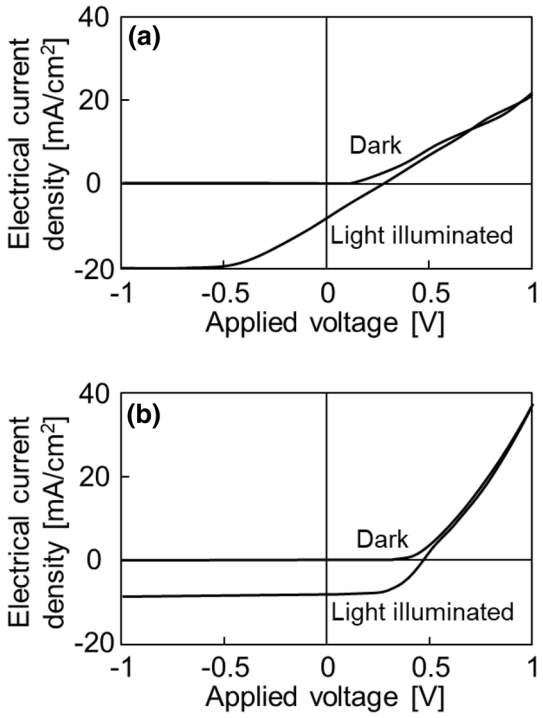

Fig. 8 J–V characteristics for the 10 Ω cm p-type samples with the top surface implanted with phosphorus atoms at **a** 200 and **b** 500 °C

phosphorus-implanted surface. Diode-rectified characteristics were observed in the J–V curves in the dark field. This means that p–n junctions were formed via activation by ion implantation under substrate heating at 200 and 500 °C. The electrical current was increased exponentially by reducing the built-in potential height by forward bias voltage application. Photo-induced current and the photovoltaic effect were observed under the AM-1.5 light illumination case, as shown in Fig. 8. The open circuit voltage was 0.24 and 0.45 V for phosphorus implantation at 200 and 500 °C, respectively. The low open circuit voltage for phosphorus implantation at 200 °C probably results from the high density of defects caused by 200 °C implantation. Photo-induced hole and electron carriers are generated in the sample by light illumination. They separate and move in the opposite directions according to the built-in potential formed below the phosphorus-doped region. The electron carriers move in the n-type doped region and the hole carriers diffuse to the p-type silicon substrate. Photo-induced electron and hole carriers are therefore accumulated at the different places in the open circuit condition. This causes the polarized voltage, which is observed as an open circuit voltage. The density of accumulation photo-induced carriers is decreased by the density of recombination defect states. Our analysis of the minority carrier effective lifetime and recombination velocity concludes that there are still many recombination defect states in the case of the 200 °C implantation as compared

with the case of 500 °C implantation. We therefore interpret that the low open circuit voltage of 0.24 V results from the high density of recombination defect states in the doped region.

4 Conclusion

Phosphorus ion implantation with a dose of 2.0×10^{15} cm^{-2} at 70 keV under substrate heating from 200 to 500 °C was investigated. Phosphorus ion implantation was carried out to the both surfaces of high resistivity crystalline silicon. The analysis of the optical reflectivity spectra of implanted surfaces revealed that the crystalline state remained in the implanted region. The effective amorphized thickness, A_{eff}, decreased from 2.9 to 1.1 nm as the implantation temperature increased from 200 to 500 °C, while A_{eff} was large for 140 nm for implantation at RT. The 9.35 GHz microwave transmittance measurement resulted in that the sheet resistivity decreased from 3700 to 470 Ω sq^{-1} as the implantation temperature increased from 200 to 500 °C, while the bare silicon substrate had 15,000 Ω sq^{-1}. 0.9-MPa-H_2O vapor-heat treatment at 250 °C for 3 h further decreased the sheet resistivity from 858 to 436 Ω sq^{-1} as the implantation temperature increased from 200 to 500 °C. The carrier mobility in the phosphorus-implanted region was obtained as 27 cm^2 V^{-1} s^{-1} by analyzing the FTIR optical absorbency spectrum for the sample implanted with phosphorus atoms at 500 °C. The carrier mobility per unit area increased 6.9×10^{13} to 4.8×10^{14} cm^{-2} with increasing substrate temperature from 200 to 500 °C. Defect passivation by 0.9-MPa-H_2O vapor-heat treatment further increased the carrier density increased from 6.9×10^{13} to 2.7×10^{14} cm^{-2} in the case of 200 °C-phosphorus implantation. Reduction of carrier trap defects is a problem for low temperature activation for implanted atoms. The photo-induced minority carrier effective lifetime increased from 2.2×10^{-6} to 1.6×10^{-4} s as the implantation temperature increased from 200 to 500 °C. The field effect passivation was achieved via activation of dopant for the case of 500 °C implantation. The rectified characteristics were obtained by current–voltage measurement in the case of phosphorus implantation to the top surface of 10 Ω cm p-type silicon substrate. Photovoltaic effect was also observed by air mass 1.5 light illumination at 0.1 W cm^{-2}. The open circuit voltage was 0.24 and 0.45 V for phosphorus implantation at 200 and 500 °C, respectively. These results show that ions implanted under low temperature heating are capable of forming p–n junctions.

References

1. M. Mehrotra, J.C. Hu, M. Rodder, Electron Devices Meeting. IEDM'99. Technical Digest. International, 5–8 Dec 1999. https://doi.org/10.1109/IEDM.1999.824183 (1999)
2. T. Ito, K. Suguro, M. Tamura, T. Taniguchi, Y. Ushiku, T. Iinuma, T. Itani, M. Yoshioka, T. Owada, Y. Imaoka, H. Murayama, T. Kusuda, 2002 Ext. Abstr. Int. Workshop on Junction Technology, p. 23 (2002)
3. A. Shima, A. Hiraiwa, Jpn. J. Appl. Phys. **45**, 5708 (2006)
4. K. Goto. T. Yamamoto, T. Kubo, M. Kase, Y. Wang, T. Lin, S. Talwar, T. Sugii, Electron Devices Meeting. IEDM'99. Technical Digest. International, 5–8 Dec 1999. https://doi.org/10.1109/IEDM.1999.824302 (1999)
5. H. Onoda, Y. Nakashima, T. Nagayama, S. Sakai, Proc. 13th Int. Workshop Junction Technology, p. 66 (2013)
6. T. Mizuno, T. Nimura, Y. Omata, Y. Nagamine, T. Aoki, T. Sameshima, Jpn. J. Appl. Phys. **56**, 04CB03 (2017)
7. K. Yasuta, M. Hasumi, T. Nagao, Y. Inouchi, T. Sameshima, The 77th JSAP Autumn Meeting, 14a-B7-2 (2016)
8. J.F. Ziegler, J.M. Manoyan, Nucl. Instrum. Methods B **35**, 215 (1988)
9. K. Asada, K. Sakamoto, T. Watanabe, T. Sameshima, S. Higashi, Jpn. J. Appl. Phys. **39**, 3883 (2000)
10. M. Born, E. Wolf, *Principles of Optics*. (Pergamon, New York, 1974) **(Chap. 1 and 13)**
11. K. Ukawa, Y. Kanda, T. Sameshima, N. Sano, M. Naito, N. Hamamoto, Jpn. J. Appl. Phys. **49**, 076503 (2010)
12. E.D. Palk, *Handbook of Optical Constants of Solids* (Academic Press, London, 1985), pp. 562–577
13. J.R. Chelikowsky, M.L. Cohen, Phys. Rev. B **10**, 5095 (1974)
14. T. Sameshima, H. Hayasaka, T. Haba, Jpn. J. Appl. Phys. **48**, 021204 (2009)
15. T. Sameshima, T. Motoki, K. Yasuda, T. Nakamura, M. Hasumi, T. Mizuno, Jpn. J. Appl. Phys. **54**, 081302 (2015)